IEEE Photonics Journal
An IEEE Photonics Society Publication

Experimental Generation of Quasi-Zero-Order Mathieu-Gauss Beams via Diffractive Elements in THz Domain

Volume 13, Number 2, April 2021

Haifeng Shi
Kejia Wang
Zhengang Yang
Jinsong Liu

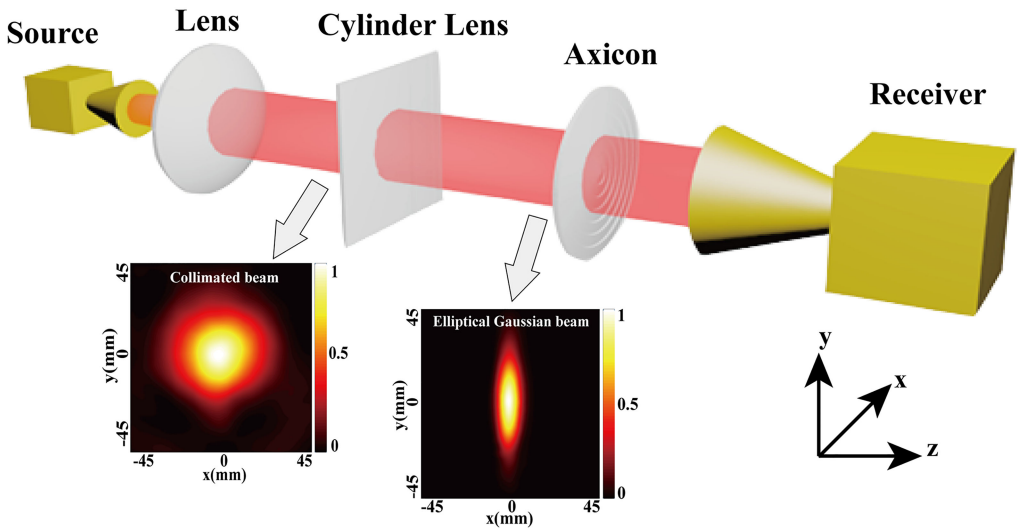

DOI: 10.1109/JPHOT.2021.3057470

Experimental Generation of Quasi-Zero-Order Mathieu-Gauss Beams via Diffractive Elements in THz Domain

Haifeng Shi,[1] **Kejia Wang**,[1] **Zhengang Yang**,[2] **and Jinsong Liu**[1]

[1]Wuhan National Laboratory for Optoelectronics, Huazhong University of Science and Technology, Wuhan 430074, China
[2]School of Optical and Electronic Information, Huazhong University of Science and Technology, Wuhan 430074, China

DOI:10.1109/JPHOT.2021.3057470

Manuscript received November 24, 2020; revised January 31, 2021; accepted February 3, 2021. Date of publication February 5, 2021; date of current version February 22, 2021. This work was supported in part by the National Natural Science Foundation of China under Grant 11574105 Corresponding author: Jinsong Liu (e-mail: jsliu4508@vip.sina.com).

Abstract: We first demonstrate the Terahertz quasi-zero-order Mathieu-Gauss beams with a 0.1-THz continuous wave. To generate these beams, two diffractive elements, a cylindrical lens and an axicon bearing specific phases are fabricated via 3D printing technology. The related numerical simulations are conducted to study intensity distributions and properties on non-diffraction and self-healing of THz quasi-zero-order Mathieu-Gauss beams in free space. Experimental results are in good agreement with numerical ones. Based on the characteristic of terahertz Mathieu-Gauss beams, they can be applied to terahertz linear array imaging system and terahertz communication.

Index Terms: Mathieu-Gauss beams, terahertz, diffractive elements.

1. Introduction

Over the past few decades, structured beams have attracted much attention in optical domain, due to their property of non-diffraction [1]–[3]. In 1987, J. Durnin *et al.* discovered Bessel beams [4], which propagate in considerably long distances without change of transverse intensities. Later, Gutiérrez-Vega proposed Cosine, Mathieu beams and Parabolic beams [5]. All these beams are based on solutions of Helmholtz wave equation in different coordinates systems, respectively. Due to its intrinsic nature, the non-diffraction beams have many applications e.g., micro particles manipulating, optical tweezer [6], [7], nonlinear optics [8], [9], and communications [10]–[13].

Since Durnin's previous work on Bessel beams, Gutiérrez-Vega was the first to demonstrate existence of Mathieu beams as a new member of the propagation-invariant optical fields(PIOFs)in elliptical cylindrical coordinate [14]. Mathieu beams are structured beams, which can be represented as superposition of a number of plane waves, whose wave vectors lie on a cone in terms of Whittaker integral in McCutchen sphere [14], whose solutions can be separated into longitudinal and transverse parts, resulting in non-diffracting property.

Inspired by the accesses to generate Bessel beams, optical Mathieu beams were realized experimentally in annular-slit element by Gutiérrez-Vega [15]. Nevertheless, the proposed method gave rise to low power efficiency since the incident illumination is blocked by the aperture to a large extent. Subsequently, Gutiérrez-Vega's group proposed other methods to generate Mathieu-beams

such as printed computer-generated holograms (CGHs) [16] and axicon-based laser resonator [17]. However, fabricating holographic plates with high precision is complicated, and the beams produced by a resonator require rather strict conditions. Both methods mentioned above are expensive and difficult to manipulate, thus, they are not very suitable techniques for generating Mathieu beams. After that, R. J. Hernández *et al.* applied a phase-only spatial-light modulator (SLM) to produce Mathieu-Gauss beams [18], which was significantly more efficient than the experimental methods used by predecessors. Based on the fact that the axicon could be an efficient element to produce Bessel beams [19], [20], Ren combined axicons with amplitude modulation to generate Mathieu beams [21].

Structured beams have been extensively studied in the optical region, however, in recent years the researches have been moved into THz domain due to some updated applications [22], [23]. S. Monk *et al.* firstly realized Bessel beams by use of axicon in THz field [20]. After that, computer-generated holograms (CGHs) were utilized to produce Bessel beams around millimeter-wave band [24]. Later, Dou demonstrated numerically that a special algorithm could improve diffraction efficiency of diffractive elements in the millimeter band [25]. The attributes of Mathieu beams are very similar to Bessel beams, but less attention is paid to the Mathieu beams in the THz domain. Furthermore, to the best of our knowledge, no experiments have been reported on the Mathieu beam within the THz range.

In this paper, based on analysis of the previous methods on generating Mathieu-Gauss beams in the optical domain, the THz Mathieu-Gauss beams, to be precise, the THz quasi-Mathieu-Gauss beams can be generated by using diffractive elements. Here, cylindrical lens and axicon as core components in experimental set were processed into wrapped phase plates via high-efficiency 3D printing technology [26], [27], which achieved the transformation of THz quasi-zero-order Mathieu-Gauss beams from mathematical model to experimental results. The experimental results show that the generated beams also have non-diffraction and self-reconstruction characteristics, which are in good agreement with the numerical ones. THz quasi-zero-order Mathieu-Gauss beams are believed to have potential advantages in THz linear array imaging and THz muti-channel communication due to their specific field distributions.

2. Theory and Fabrication of Phase Plates

Any non-diffracting beams can be represented as superposition of a group of plane waves whose vectors exist in the form of cone. Based on solutions of Helmholtz equation in terms of Whittaker integral [28], the fields can be expressed as follows:

$$U(\rho, \phi, z) = \exp(ikz) \int_0^{2\pi} A(\theta) \times \exp[ik_t \rho \cos(\theta - \phi)]\, d\theta \tag{1}$$

where $A(\theta)$ is the complex angular spectrum function, $k_t = k_0 \sin\alpha$ and $k_z = k_0 \cos\alpha$ represent magnitudes of the transverse and the longitude components of wave-vector k_0 , respectively. For Mathieu function, the angular spectrum $A(\theta)$ is determined by angular Mathieu function, and the zero-order mode can be expressed as follows:

$$ce_{2n}(\eta, q) = \sum_{j=0}^{\infty} A_{2j}^{(2n)}(q) \cos 2j\eta \tag{2}$$

replacing $A(\theta)$ by ce_{2n} [28], [29], the solution of (1) is expressed as follows:

$$uc_{2n}(\rho, \phi, q, z) = \sum_{j=0}^{\infty} A_{2j}^{(2n)}(q)(-1)^j \cos(2j\phi) J_{2j}(k_t \rho) \tag{3}$$

where the coefficients $A_{2j}^{(2n)}(q)$ are equal to values of eigenvectors of the matrixes generated by each values of q, and uc_{2n} is zero-order radial Mathieu function. Here, q is the elliptical parameter of the Mathieu function, which is defined as $q = h^2 k_t^2/4$, where $2h$ is the interlocal separation [29].

The distributions of Mathieu functions are equal to those of Mathieu beams and the beams are non-diffracting beams with no energy loss during propagation ideally. Thus, the plane waves modulated by angular Mathieu functions are theoretically essential to evolve Mathieu beams. However, on this basis, it is almost impossible to obtain these modulated plane waves experimentally. Then Gutiérrez-Vega proposed that one-dimensional Gaussian function can approximately replace zero-order angular Mathieu function [30]. Accordingly, the choice of elliptic Gaussian function in place of one-dimensional Gaussian function is almost subtly adopted. Therefore, it is essential to generate elliptical Gaussian plane-wave beams equally whose distributions are given by:

$$U(x, y, z) = U_0 \exp\left(-\frac{x^2}{\omega_{x0}^2(z)} - \frac{y^2}{\omega_{y0}^2(z)}\right) \tag{4}$$

where ω_{0x} and ω_{0y} are the waist radius of the elliptical beam at two different directions along x and y. By setting (4) into (1) through coordinate transformation, we can obtain the calculated results, whose distributions may be approximate to profiles of zero-order Gauss-Mathieu radial function. Hence, the beams generated from these distributions could be named quasi-zero-order Mathieu-Gauss beams.

Producing these beams is mathematically accessible, and what is more, it is significant to implement them experimentally. Here, cylindrical lens and axicon are combined to produce elliptical Gaussian beam and quasi-zero-order Mathieu-Gauss beam, successively, which can be used flexibly and make the beams transform well from theory to reality. In our designs, in order to produce quasi-zero-order Gauss-Mathieu beams in THz domain, we applied 3D printed technology to fabricate phase plates since it can process phase-plates quickly and accurately. Here, the main parameters of 3D printer (Union Tech Inc., Lite450) are described, where the printing resolution in lateral xy-plane and direct z-axis correspond to 100 μm and 50 μm respectively. The 3D material used is photosensitive resin (LY1101), whose refractive index and absorption coefficient are 1.6 and 0.49 cm^{-1} at 0.1 frequency of THz, respectively, and derived from Zomega-Z3 time domain spectrometer (THz-TDS).

Considering the obvious absorption in propagation, the refractive elements are not suitable for generating structure beams in THz waveband. Inspired by the previous work, the phase devices can be made into diffractive elements based on the equivalence between optical path and phase-shift. In our designs, cylindrical lens and axicon are core elements, and their phases are respectively written as follows:

$$\phi_1(x, y) = \sqrt{R^2 - x^2} - \sqrt{R^2 - d^2} \tag{5}$$

$$\phi_2(x, y) = \left(r_0 - \sqrt{x^2 + y^2}\right) \tan\gamma \tag{6}$$

where R is radius of curvature of cylindrical lens, d is half width size of it at sagittal direction, r_0 and γ are radius and basic angle of the axicon, respectively. Similarly, both cylindrical lens and axicon can be processed into diffractive elements, wrapped elements, resulting in low material absorption to THz waves and keeping a good beam-shape in comparison with refractive elements. According to the principle mentioned above, cylindrical lens and axicon can be compressed quite thin, with the phase distributions between [0, 2 π]. As the beams pass through homogeneous material with thickness of h , the phase shift can be obtained, as $\Delta\phi = 2\pi(n - 1)h/\lambda$, where n is the refractive index of the material, λ is wavelength of the beams. According to this, the height profiles of wrapped cylindrical lens and axicon can be expressed as follows:

$$h_1(x, y) = \mathrm{mod}_{\frac{\lambda}{n-1}}\left[\frac{\lambda\phi_1(x, y)}{2\pi(n - 1)}\right] + h_0 \tag{7}$$

$$h_2(x, y) = \mathrm{mod}_{\frac{\lambda}{n-1}}\left[\frac{\lambda\phi_2(x, y)}{2\pi(n - 1)}\right] + h_0 \tag{8}$$

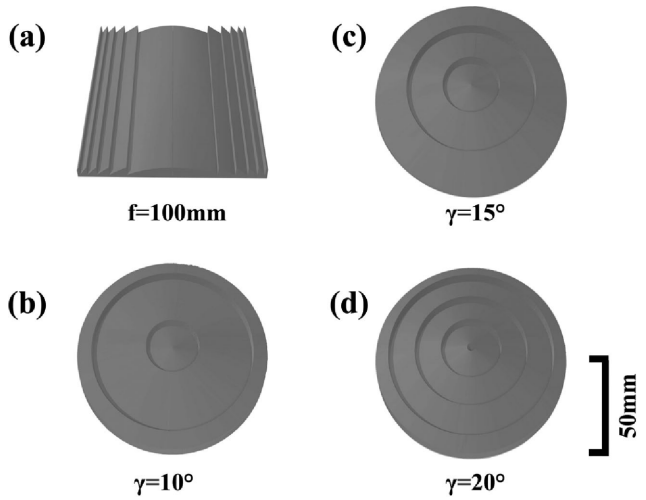

Fig. 1. The profiles of model in diffractive elements, (a) wrapped cylindrical lens with focal length $f =$ 100 mm, (b, c, d) wrapped axicons with basic angles $\gamma = 10°, 15°, 20°$.

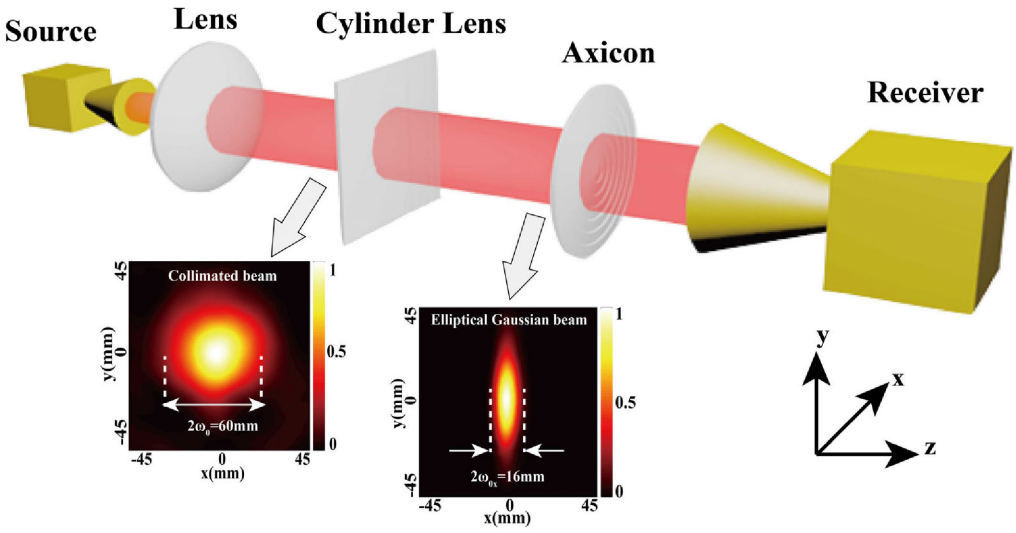

Fig. 2. Schematic diagram of experimental setup for generating THz quasi-zero-order Mathieu beam. The left inset: the normalized intensity distribution of the collimated THz beam, the right inset: the normalized intensity distribution of the elliptical Gaussian beam.

where h_0 is 2 mm, the basic thickness of phase plates. The corresponding models of wrapped cylindrical lens and axicons with specific parameters originally obtained from Matlab(numerical simulation software) are shown in Fig. 1.

The THz quasi-zero-order Mathieu beam can be normally generated by the diffractive elements, the wrapped cylindrical lens and the axicon, which is the realization of Whitaker's integral in experimentally.

3. Experimental Generation and Results of Quasi-Zero-Order Mathieu-Gauss Beams

The map of experimental setup is shown in Fig. 2. The THz transmitter consists of Gunn diode (Spacek Labs Inc.), whose outpower is 80 mW and radiates 0.1 THz continuous wave and the

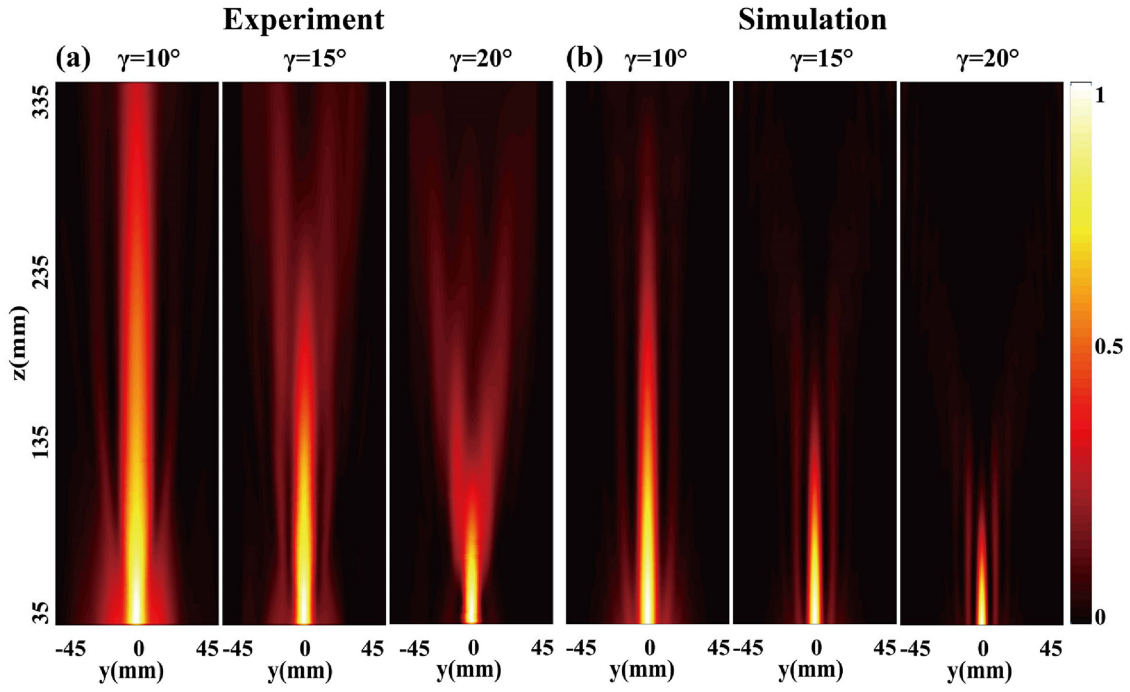

Fig. 3. The normalized intensity distributions of the generated THz quasi-zero-order Mathieu-Gauss beams in yz-plane. (a) Experimental results, (b) numerical simulation results.

diagonal horn antenna emits THz wave to free space. The convex lens to generate collimated THz beam is a commercial product, which is compound of high-density polyethylene (HDPE). The THz receiver is Schottky diode (Virginia Diode Inc.) with the same skeleton to transmitter. It is fixed on a motorized three-dimensional translation stage, where the size of detection area is 90 mm$\times$300 mm in yz-plane and 90 mm$\times$90 mm in xy-plane, respectively.

The left inset of Fig. 2 represents the normalized intensity distributions of the incident THz beam, namely the collimated beam, whose intensity profiles approximate to Gaussian beam. Here, the width of beam is $2\omega_0 = 60$ mm , where ω_0 corresponds to waist radius on the Gaussian beam. The Gaussian beam is converted to an elliptical Gaussian beam by means of a cylindrical convex lens with a focal length ($f = 100$ mm). That is caused by beam compressing only in x direction, showing the double waist radius in the elliptical Gaussian beam coupled with $\omega_{0x} = 8$ mm, $\omega_{0y} = 30$ mm respectively. The elliptical Gaussian beam is used as an incident beam to enter the wrapped axicon for generating quasi-zero-order Mathieu-Gauss beam.

For comparison, we properly picked a set of wrapped axicons with basic angles of 10°,15° and 20° respectively to study the properties of the generated THz quasi-zero-order Mathieu-Gauss beams. As shown in Fig. 3(a), the experimental normalized intensity distributions of the generated beams are recorded in yz-plane. It is assumed that original point, x = 0 mm, y = 0 mm and z = 0 mm are located at the vertex of axicon. However, the actual detected point is from z = 35 mm originally, because the top of the horn cannot touch the defined initial coordinates due to the horn structure. It is apparent that the generated quasi-zero-order Mathieu-Gauss beams demonstrate non-diffracting property. The main lobes of the beams appear to be a type of ray that scarcely diverge over a considerable propagation distances, and the side symmetric lobes are darker than the mains. Evidently, with the decrease of the basic angle of the wrapped axicon, the non-diffraction lengths of the generated beams gradually lengthen. In Fig. 3(b), the normalized intensity distributions of the generated beams from numerical simulations based on angular spectrum theory are demonstrated. Obviously, the features of the observed beams are similar to those represented in the simulations, while the details between them differ to some degree. For

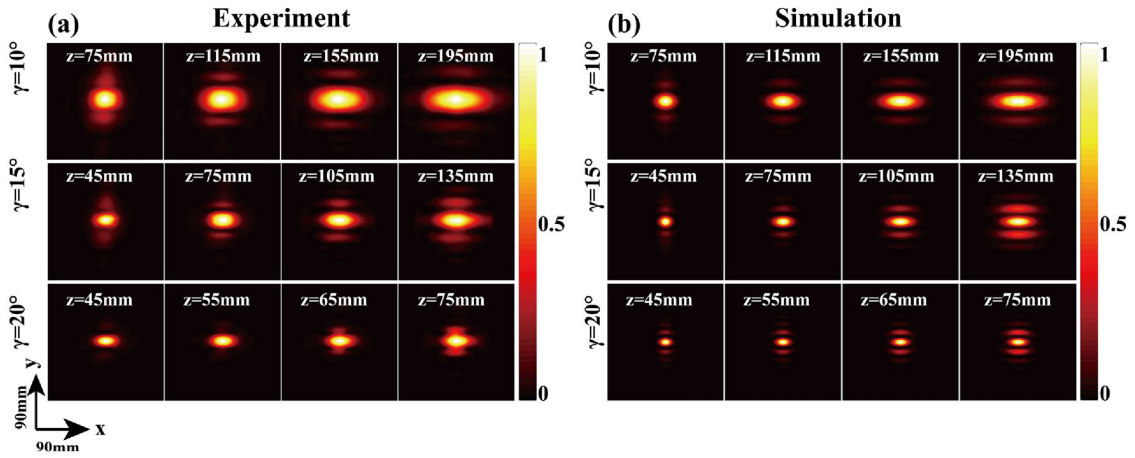

Fig. 4. The normalized intensity distributions of THz quasi-zero-order Mathieu-Gauss beams generated from each basic angle diffractive axicon at different positions along propagation direction. (a) Experimental results, (b) numerical simulation results.

instance, the main lobes in the experiments are slightly broader than in the simulations, and the non-diffraction length appears to be longer than in the simulation. This may be due to experimental system aberration and beam diffusion as a result of imperfect Gaussian beam from the emitter. Nevertheless, the experimental results are still in accordance with the simulations in terms of the dynamic characteristics in the beams.

Similarly, Fig. 4 shows the experimental and simulated transverse normalized intensity distributions of the xy plane at different positions corresponding to the yz plane. The transverse profiles clearly show a stipe-structures in which the main lobe appears to be the brightest elliptic fragment surrounded by a brighter side lobe symmetrically such as the crescent fringes. Owing to the non-circular symmetry of the elliptical Gaussian beam, non-diffracted regions of different sizes are formed in xz and yz planes after the beam is focused by axicon, resulting in the specific transverse distribution due to different divergence of the beam along in x and y axis. This distribution corresponds to the yz plane. Simultaneously, it is also observed that with the extension of propagation distances along the z axis, the brightness contrast between the main lobes and the side lobes tends to diminish, as shown in Fig. 4. These results can be attributed to modulation of the envelops of elliptical Gaussian-beams with divergent trend. For each diffractive element, with increase of parameter γ , the related ranges of quasi-invariant field distributions with stripe-structure become decreased gradually. This corresponds to the tendency that the relevant non-diffraction lengths become shorter. It could be traced to the root that a larger basic angle will lead to the shortening of the longitudinal length and the loss of field energy in the corresponding rhombic region shaped by overlapping of the generated beams. Observed roundly, the transverse normal intensity distributions in the experiments are consistent with those in the simulations, though there are somewhat differences in the detailed shapes of the field distributions. That may be due to the imperfect Gaussian profiles of the original beam and the aberrations produced by the diffractive elements of the system.

Fig. 5 presents plots of the transverse normalized intensity along the y-axis of the quasi-zero-order Mathieu-Gauss beams at different positions corresponding to Fig. 4. Meanwhile, the parameter q in (3) above is an important factor embodying the characteristics of quasi-zero-order Mathieu-Gauss beams. Each graph is composed of three different curves. The blue solid lines and the green solid lines correspond to the experimental and numerical simulation results respectively, and then the red dotted lines fit the curves of the zero-order Mathieu-Gauss functions according to various values of q. There are some differences in profiles between simulated and experimental curves, and the reasons for them are similar with the mentioned above. The connections between

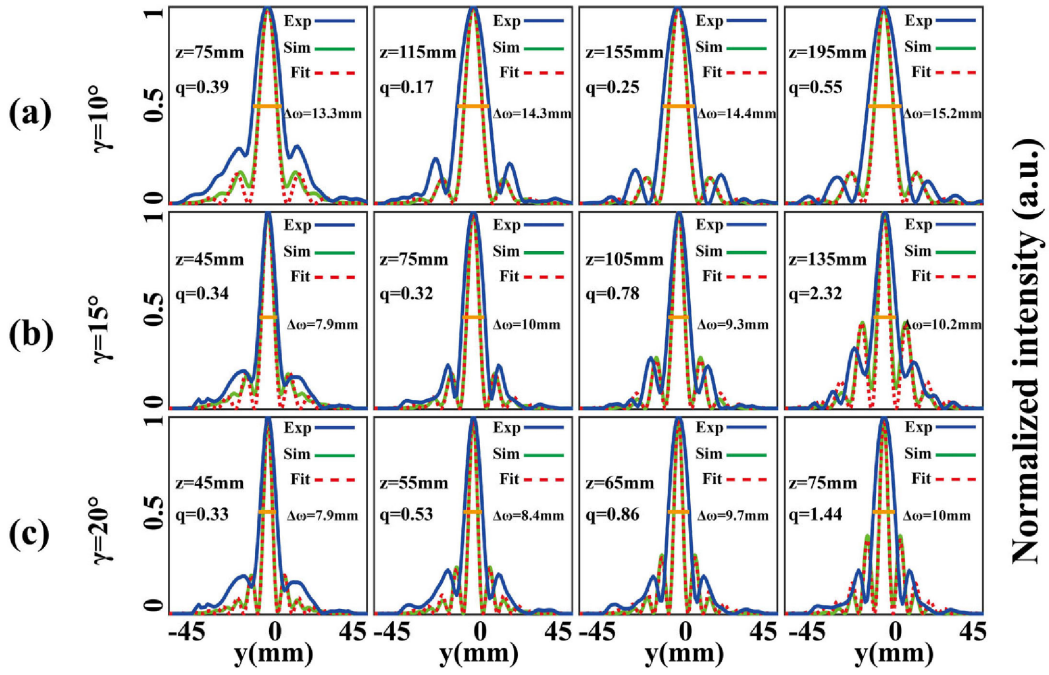

Fig. 5. The normalized intensity curves of the generated THz quasi-zero-order Mathieu-Gauss beams at different positions along propagation direction. (a) The diffractive axicon with $\gamma = 10°$, (b) the diffractive axicon with $\gamma = 15°$, (c) the diffractive axicon with $\gamma = 20°$.

parameters q and the evolution of the quasi-zero-order Mathieu-Gauss beams are clearly illustrated in Fig. 5. For each row of the graphs, as the propagation distances increase, the q values combined with the corresponding normalized intensity profiles tend to be larger generally despite the descending order of q in the first two column. This can be attributed to the fact that the profiles of the generated beams at the initial propagation distances are hardly to approach the Mathieu beams, resulting in abnormal fitting values. After that, the q value shows an upward trend since the diverging elliptical Gaussian-beams mainly lead to the augment of k_t value. Likewise, the intensities of central peaks against shoulder peaks on the curves appear to decrease somewhat, while from $\Delta\omega$(FWHM), the main lobes just show slight divergence, showing non-diffracting characteristics of the THz quasi-zero-order Mathieu-Gauss beams.

In addition, the generated THz quasi-zero-order Mathieu-Gauss beams also demonstrate the self-healing properties similar to other structured beams [31], [32] to intrigue one's interests. To study this property, the diffractive axicon corresponding to $\gamma = 15°$ was arbitrarily selected to verify that, and there is no exclusivity. A thin circular metal segment with a radius of 6 mm is placed behind the central aperture of the diffractive axicon to partially block the generated Mathieu-Gauss beams. Fig. 6(a, b) shows the propagation process of the blocked Mathieu-Gauss beams in experiments and numerical simulations at yz-plane respectively. In Fig. 6(a), due to the horn structure, there is an undetected area, so the first 35 mm propagation distance is omitted. Fig. 6(c, d) shows the transverse normalized intensity distributions at different positions in the experiments and calculations, and Fig. 6(e) presents the wrapped axicon sticked with a circle copper. In Fig. 6(b), the beams generated by blocking show the first 10 mm deformities along the propagation direction. Once beyond this range, the shapes of these beams are similar to that of the unblocked beams, though the main lobes of the recovered beams appear narrower than the normal beams shown above. Although partially disturbed during the primary propagation, once beyond this stage, the beams can reconstruct themselves to gradually close the structures without hindrance, and still retain their non-diffracting character. This can be explained by the fact that the generated beam passing through the diffractive axicon may continue to propagate to form the quasi-Mathieu-Gauss beam in

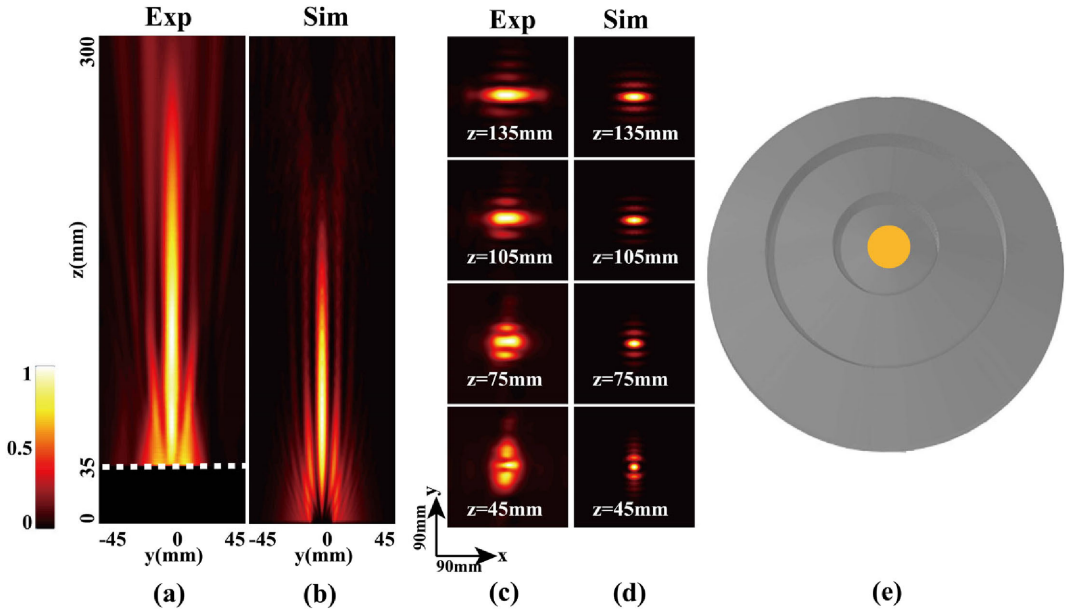

Fig. 6. (a) Experimental normalized intensity distribution of the generated THz quasi-zero-order Mathieu-Gauss self-healing beam in yz-plane, (b) corresponding simulation results (c) Experimental normalized intensity distributions of the generated self-healing beam in xy-plane at different positions along propagation direction, (d) corresponding simulation results. (e) The wrapped axicon with a thin metal wafer whose radius is 6 mm.

the rhombic region formed by the overlapping of the beams. Similarly, it can be deduced that the deformities of the beam are likely to occur during the experiments. The results corresponding to the numerical calculations are generally consistent with the experimental results, while some of the differences between the two may be related to the source beam defects and aberrations caused by the above elements.

4. Conclusion

In this paper, the terahertz quasi-zero-order Mathieu-Gauss beams with a frequency of 0.1 THz have been produced via a set of effective experimental methods and the two diffractive elements, including 3D-printed wrapped cylindrical lens and axicon. The generated THz quasi-zero-order Mathieu-Gauss beams demonstrated a good property of non-diffraction in some degree. Specifically, as the parameter γ on the diffractive axicon becomes smaller, the non-diffraction lengths of the beams extend longer. Meanwhile, the transverse intensity profiles of the beams correspond to q parameters with different values at different positions along the propagation direction. In addition, the self-healing properties of quasi-zero-order Mathieu-Gauss beams are also revealed. The beams blocked by a segment can be rebuilt by themselves after a process of propagation, and they are also non-diffracting. The corresponding numerical simulations remain in content agreement with experimental results. Noteworthily, the generated THz quasi-zero-order Mathieu-Gauss beams could be utilized to play a key role in the fields of THz line-array imaging and communications in the future.

References

[1] M. A. Porras, "Diffraction-free and dispersion-free pulsed beam propagation in dispersive media," *Opt. Lett.*, vol. 26, no. 17, pp. 1364–1366, Sep. 2001.

[2] L. Niggl and M. Maier, "Gain-guided modes in stimulated scattering processes with diffraction-free pump beams," *Opt. Commun.*, vol. 154, no. 1–3, pp. 65–69, Aug. 1998.
[3] K. Kono, M. Irie, and T. Minemoto, "Generation of nearly diffraction-free beams using a new optical system," *Opt. Rev.*, vol. 4, no. 3, pp. 423–428, May/Jun. 1997.
[4] J. Durnin, J. Miceli Jr., and J. H. Eberly, "Diffraction-free beams," *Phys. Rev. Lett.*, vol. 58, no. 15, pp. 1499–1501, Apr. 1987.
[5] J. C. Gutierrez-Vega and M. A. Bandres, "Helmholtz-Gauss waves," *J. Opt. Soc. Amer. A.*, vol. 22, no. 2, pp. 289–298, Feb. 2005.
[6] M. Horodynski *et al.*, "Optimal wave fields for micromanipulation in complex scattering environments," *Nat. Photon.*, vol. 14, no. 3, pp. 149–14+, Mar. 2020.
[7] J. Tang, L. J. Yang, B. H. Liu, and Y. Wang, "Nano-particle manipulated with near-field optical tweezers," *Adv. Mater. Res-Switz*, vol. 299–300, pp. 1068–106+, 2011.
[8] F. W. Ye, D. Mihalache, and B. B. Hu, "Elliptic vortices in composite mathieu lattices," *Phys. Rev. A.*, vol. 79, no. 5, pp. 1–7, May 2009.
[9] O. Cohen *et al.*, "Observation of random-phase lattice solitons," *Nature*, vol. 433, no. 7025, pp. 500–503, Feb. 2005.
[10] N. Mphuthi, L. Gailele, I. Litvin, A. Dudley, R. Botha, and A. Forbes, "Free-space optical communication link with shape-invariant orbital angular momentum bessel beams," *Appl. Opt.*, vol. 58, no. 16, pp. 4258–4264, Jun. 2019.
[11] J. Peng, L. Zhang, K. C. Zhang, and J. X. Ma, "Channel capacity of OAM based FSO communication systems with partially coherent bessel-gaussian beams in anisotropic turbulence," *Opt. Commun.*, vol. 418, pp. 32–36, Jul. 2018.
[12] Y. S. Yuan *et al.*, "Beam wander relieved orbital angular momentum communication in turbulent atmosphere using bessel beams," *Sci Rep-Uk*, vol. 7, pp. 1–7, Feb. 2017.
[13] J. Du *et al.*, "Demonstration of M-ary encoding/decoding using visible-light bessel beams carrying orbital angular momentum (OAM) for free-space obstruction-free optical communications," in *Proc. Opt. Fiber Commun. Conf. Exhib.*, 2015, pp. 1–3.
[14] J. C. Gutierrez-Vega, M. D. Iturbe-Castillo, and S. Chavez-Cerda, "Alternative formulation for invariant optical fields: Mathieu beams," *Opt. Lett.*, vol. 25, no. 20, pp. 1493–1495, Oct. 2000.
[15] J. C. Gutierrez-Vega *et al.*, "Experimental demonstration of optical mathieu beams," *Opt. Commun.*, vol. 195, no. 1–4, pp. 35–40, Aug. 2001.
[16] S. Chavez-Cerda *et al.*, "Holographic generation and orbital angular momentum of high-order mathieu beams," *J. Opt. B-Quantum S. O.*, vol. 4, no. 2, pp. S52–S57, Apr. 2002.
[17] M. B. Alvarez-Elizondo, R. Rodriguez-Masegosa, and J. C. Gutierrez-Vega, "Generation of mathieu-gauss modes with an axicon-based laser resonator," *Opt. Exp.*, vol. 16, no. 23, pp. 18770–18775, Nov. 2008.
[18] R. J. Hernandez-Hernandez, R. A. Terborg, I. Ricardez-Vargas, and K. Volke-Sepulveda, "Experimental generation of mathieu-gauss beams with a phase-only spatial light modulator," *Appl. Opt.*, vol. 49, no. 36, pp. 6903–6909, Dec. 2010.
[19] T. J. Du, T. Wang, and F. T. Wu, "Line focusing characteristics of axicon illuminated by non-diffracting bessel beam," (in Chinese), *Acta. Phys. Sin-Ch Ed.*, vol. 62, no. 13, pp. 1–6, Jul. 2013.
[20] S. Monk, J. Arlt, D. A. Robertson, J. Courtial, and M. J. Padgett, "The generation of bessel beams at millimetre-wave frequencies by use of an axicon," *Opt. Commun.*, vol. 170, no. 4–6, pp. 213–215, Nov. 1999.
[21] Z. Ren, H. Hu, and B. Peng, "Generation of mathieu beams using the method of 'combined axicon and amplitude modulation'," *Opt. Commun.*, vol. 426, pp. 226–230, 2018.
[22] W. Shao, S. J. Huang, X. P. Liu, and M. S. Chen, "Free-space optical communication with perfect optical vortex beams multiplexing," *Opt. Commun.*, vol. 427, pp. 545–550, Nov. 2018.
[23] H. F. Meng, B. Xiang, J. L. Zhang, W. B. Dou, and Y. Z. Yu, "The generation of bessel beam and its application in millimeter wave imaging," *J. Infrared Millim. Te.*, vol. 35, no. 2, pp. 208–217, Feb. 2014.
[24] J. Salo *et al.*, "Millimetre-wave bessel beams using computer holograms," *Electron. Lett.*, vol. 37, no. 13, pp. 834–835, Jun. 2001.
[25] Y. Z. Yu and W. B. Dou, "Nondiffracting millimeter waves beams generated by diffractive optical elements," in *Proc. Eur. Microw. Conf.*, 2008, vol. 1–3, pp. 29–32.
[26] C. M. Liu, L. T. Niu, K. J. Wang, and J. S. Liu, "3D-printed diffractive elements induced accelerating terahertz Airy beam," *Opt. Exp.*, vol. 24, no. 25, pp. 29343–U1209, Dec. 2016.
[27] X. L. Wei *et al.*, "Generation of arbitrary order bessel beams via 3D printed axicons at the terahertz frequency range," *Appl. Opt.*, vol. 54, no. 36, pp. 10641–10649, Dec. 2015.
[28] A. Chafiq, Z. Hricha, and A. Belafhal, "Paraxial propagation of mathieu beams through an apertured ABCD optical system," *Opt. Commun.*, vol. 253, no. 4–6, pp. 223–230, Sep. 2005.
[29] A. Chafiq, Z. Hricha, and A. Belafhal, "A detailed study of mathieu-gauss beams propagation through an apertured ABCD optical system," *Opt. Commun.*, vol. 265, no. 2, pp. 594–602, Sep. 2006.
[30] J. C. Gutierrez-Vega, M. D. Iturbe-Castillo, and S. Chavez-Cerda, "Alternative formulation for invariant optical fields: Mathieu beams," *Opt. Lett.*, vol. 25, no. 20, pp. 1493–1495, Oct. 2000.
[31] M. Anguiano-Morales, "Self-healing properties of asymmetric bessel beams," *Opt. Quant. Electron.*, vol. 50, no. 10, Oct. 2018.
[32] J. D. Ring, J. Lindberg, A. Mourka, M. Mazilu, K. Dholakia, and M. R. Dennis, "Auto-focusing and self-healing of pearcey beams," *Opt. Exp.*, vol. 20, no. 17, pp. 18955–18966, Aug. 2012.